PHOTOCATALYTIC DEGRADATION OF 4-CHLOROPHENOL BY •OH RADICALS GENERATED BY THIOPHENE OLIGOMERS INCORPORATED IN ZSM-5 ZEOLITE CHANNELS

Gabriel Čík[a1,*], Milada Hubinová[a2], František Šeršeň[b], Jozef Krištín[c] and Monika Antošová[d]

[a] *Department of Environmental Engineering, Faculty of Chemical and Food Technology, Slovak University of Technology, 812 37 Bratislava, Slovak Republic; e-mail: [1] cik@chtf.stuba.sk, [2] hubinova@chtf.stuba.sk*

[b] *Institute of Chemistry, Faculty of Natural Sciences, Comenius University, 842 15 Bratislava, Slovak Republic; e-mail: sersen@fns.uniba.sk*

[c] *Central Laboratory of Electronic and Optical Methods, Faculty of Natural Sciences, Comenius University, 842 15 Bratislava, Slovak Republic; e-mail: kristin@fns.uniba.sk*

[d] *Department of Chemical and Biochemical Engineering, Faculty of Chemical and Food Technology, Slovak University of Technology, 812 37 Bratislava, Slovak Republic; e-mail: antosova@cvt.stuba.sk*

Received April 22, 2003
Accepted August 1, 2003

Degradation of 4-chlorophenol by reactive oxygen species was studied, the latter being generated by photo-assisted reactions of thiophene oligomers, synthesized in channels of the Na-ZSM-5 zeolite. The photoreaction was carried out in an aqueous suspension of photocatalyst, irradiated with visible light ($\lambda > 400$ nm). The spin-trapping method was used to detect the generated •OH radicals. The main products of the photodecomposition of 4-chlorophenol were found to be phenol, hydroquinone and maleic acid.

Keywords: ZSM-5 zeolite; Polythiophenes; Reactive oxygen species; 4-Chlorophenol; Photochemistry; Heterogeneous catalysis; Dehalogenation; Green chemistry; Photolysis.

Oxidative decomposition and transformation of organic substrates with oxygen using photocatalysts is one of the most frequently used methods for purification of waste waters. Among these methods photocatalytic reactions on semiconductor powders are of great interest because of a large variety of pollutants[1,2]. During photocatalytic processes, photoinduced electrons and holes can reduce and oxidize species adsorbed on semiconductor particles[2]. One of the semiconductors most widely used as a photocatalyst, triggering the oxidative destruction and mineralization of organic substrates, is TiO_2. Due to the width of the band gap of TiO_2 (3.2 eV), the processes of catalytic

doi:10.1135/cccc20032219

oxidative destruction are accomplished upon irradiation with UV light, when only approximately 4% of the solar radiation is effective.

Anchoring of pigments, in particular phthalocyanine complexes on wide-band gap semiconductors[3–6], is an alternative method in which a dye (sensitizer) adsorbed on TiO_2 surface gets excited by absorbing visible light and an intercomponent electron transfer takes place in the couple molecular semiconductor–TiO_2.

On the other hand, it has been reported that π-conjugated poly(arylene)s (organic semiconductors with $\lambda_{max} > 400$ nm), such as poly(1,4-phenylene), poly(pyridine-2,5-diyl), and poly(2,2′-bipyridine-5,5′-diyl), make possible photocatalytic reduction of water, ketones, and CO_2 in the presence of triethylamine as a sacrificial electron donor[7–9]. As a first application of π-conjugated polymers to the degradation of water pollutants, photocatalytic degradation of four agrochemicals using poly(3-octylthiophene-2,5-diyl) and poly[2,5-bis(hexyloxy)-1,4-phenylene] films under gas bubbling (oxygen) and UV light irradiation was investigated[10]. Since the poly(3-octylthiophene-2,5-diyl) film possesses a strong absorption band at $\lambda_{max} = 504$ nm, it can be activated by visible light. Therefore, the visible-light-induced catalytic degradation of a fungicide (iprobenfos) using a poly(3-octylthiophene-2,5-diyl) film, by varying the oxygen pressure of bubbling gases can be used[11,12].

In our earlier work[13], we have found that thiophene oligomers, serving as models of conducting polythiophenes embedded in the channels of zeolite ZSM-5 structure, generate in aqueous media electrons, when irradiated by visible light, ultimately producing superoxide ($O_2^{\bullet -}$) and H_2. This finding inspired us to design a heterogeneous photocatalytic system (thiophene oligomers–ZSM-5 zeolite) for photolytic degradation of selected pollutants (4-chlorophenol) by visible light. We now present the results of the study of photocatalytic degradation of 4-chlorophenol as a model chlorinated contaminant of the environment. The study concentrated on identification of the reactive oxygen species (ROS), participating in decomposition reactions proceeding in aqueous media and degradation products of 4-chlorophenol.

EXPERIMENTAL

Oxidation polymerization (oligomerization) of thiophene was performed in channels of the Na-ZSM-5 zeolite (VURUP Co., Slovak Republic) after ion exchange of Fe^{3+} for Na^+ according to our previous work[13]. The exchanged Fe^{3+}-ZSM-5 was prepared by refluxing (4 h) 5 g of zeolite with 100 cm^3 of aqueous 0.3 M $FeCl_3 \cdot 6H_2O$ (Aldrich).

The X-ray microanalysis of zeolite samples was conducted by scanning electron microscopy with a JXA-840 A instrument (JEOL). The synthesized sample contained 0.1 wt.% Fe and 3.1 wt.% S. The morphology of zeolites was studied by the analytical transmission microscope JEOL, model TEM 2000FX equipped with an ASID 20 and energy-dispersive probe Link AN 10000. Transmission electrons were generated by electron gun with acceleration of 160 kV; resolution 0.28 nm. Photographic records were made on Kodak film sheets. For direct observation by TEM, zeolite sample were pretreated by the following procedure: some 0.01 g of a sample was mixed with 100 cm^3 of ethanol and homogenized in an ultrasound apparatus (Power Sonic PS 01000, NOTUS-P.S. Co., Vrable, Slovakia) during 10 min. Finely suspended particles of zeolite in alcohol were transferred with a micropipette on to a copper mesh with mesh size 10 × 10 μm, on which a graphite layer of 5–10 nm was previously deposited. Vacuum deposition was used to cover dry samples (24 h at 40 °C *in vacuo*) with another layer of *ca* 5 nm of graphite. The pretreated samples produced images allowing assessment of iron distribution in zeolite after ion exchange.

EPR spectra were measured with an ERS-230 apparatus (ZWG, Academy of Sciences, Germany) in the X-region at microwave output 5 mW and modulation amplitude 0.5 mT. As a $^1O_2$ (singlet oxygen) and $O_2^{\bullet -}$ detector, 2,2,6,6-tetramethylpiperidine (TEMP, synthesized by Dr D. Végh, Department of Organic Chemistry, Slovak University of Technology; 99.3%, 1.4 × 10^{-4} mol dm^{-3}) was used. The 5,5-dimethyl-4,5-dihydroxypyrrole *N*-oxide (DMPO, Sigma) was used as spin trap (3.4 × 10^{-4} mol dm^{-3}). Samples (water suspension of the treated zeolite at pH 5.63) were irradiated with a metal-halogen lamp (250 W, Tesla, ≈60 W m^{-2}) from the distance of 50 cm through a 5-cm water filter in the cavity of the EPR apparatus at 25 °C.

The photodegradation of 4-chlorophenol and phenol was carried out in a magnetically stirred round-bottom flask (250 cm^3). The reaction mixture (pH 5.6) was composed of 250 cm^3 of an aqueous solution of the reactant (2.5 × 10^{-3} mol dm^{-3}) and 250 mg of photocatalyst. For irradiation, a metal-halogen lamp (150 W, Osram, ≈35 W m^{-2}) was placed about 30 cm from the reaction flask, its light being filtered with 10-cm aqueous filter kept at 25 °C.

The analysis of photodecomposition products were performed by high-performance liquid chromatography (HPLC). The HPLC system consisted of a pump Maxi-Star K-1000, an on-line degasser Model A1050, a refractive index (RI) detector Type 298.00, an injector valve equipped with a 10-mm^3 loop, all from Knauer (Berlin, Germany), and a column thermostat Jetstream Plus II (Therotechnic Products, Germany). Separation was carried out using a Tessek column, model CGX C18 (150 mm × 3 mm i.d.; Tessek, Prague, Czech Republic). As a mobile phase, 50% ethanol in redistilled water was used at a flow rate of 0.5 cm^3 min^{-1}. The column temperature was set to 25 °C. The RI detector was operated at 25 °C. The chromatographic data were recorded and evaluated using the EuroChrom 2000 Integration Package Software (Knauer, Berlin, Germany).

RESULTS AND DISCUSION

As can be seen from Fig. 1a showing a TEM image of the Na-ZSM-5 crystal, prior to exchange of Fe^{3+} for Na^+ the crystal remains smooth, without visible changes or perturbations (*cf*. the TEM image in Fig. 1b showing Fe-ZSM-5 after ion-exchange). Dark spots of various sizes can clearly be

identified (ranging from 5 to about 50 nm). These "morphological" changes are attributed either to clusters of various Fe forms aggregated after exchange for Na^+, or to surface defects containing larger clusters of Fe ions.

Figure 2 shows records of analysis of a Fe^{3+}-ZSM-5 sample after oligomerization of thiophene, whereby Fig. 2a represents analysis of zeolite surface without visible defects, whereas Fig. 2b shows analysis of the faulted zeolite surface. It appears that Fe^{3+} ions are found predominantly in the channels of zeolite, or in surface defects. Such faults are ion clusters of various sizes (Fe_2O_3; Fe^{3+}–O–Fe^{3+}), as has already been assumed in our earlier report[14] (higher Fe content on the "defect" surface – Fig. 2b; *cf*. Fe/Si). Sample

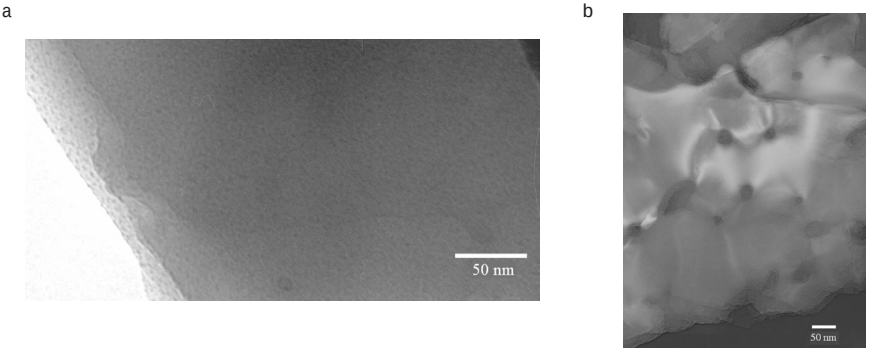

FIG. 1
TEM image of a Na-ZSM-5 zeolite crystal (a); TEM image of a Fe-ZSM-5 crystal (b)

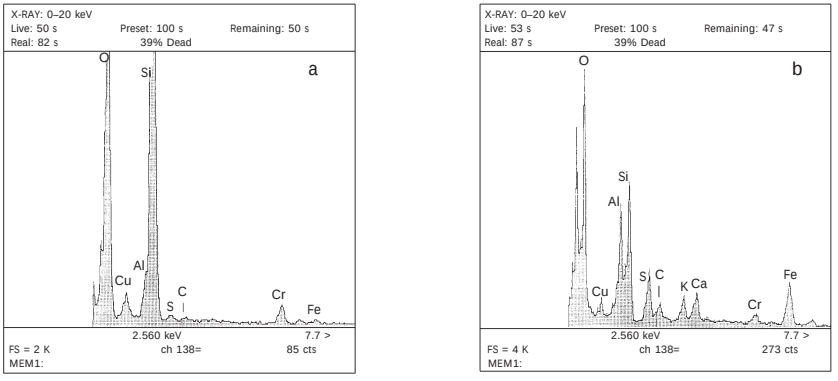

FIG. 2
Analysis of upper layers of a Fe-ZSM-5 crystal, doped with thiophene oligomers, obtained in the region without visible morphological perturbations (a) and in the region with higher incidence of morphological disturbances (b)

2b also contains more sulfur suggesting that oligomerization of thiophene took place mainly in parts with higher concentrations of Fe^{3+} ion clusters. Thus it appears that the photocatalytically active locations of thiophene oligomers follow no pattern; in addition to being in regular zeolite channels, they are "bound" to irregularly distributed surface clusters of Fe ions, created after ion-exchange.

Figure 3 shows time-dependent photogeneration of superoxide (or $^1O_2$) during irradiation with visible light, monitored by oxidation of TEMP (spin-trap) in a mixture of dimethyl sulfoxide (DMSO)/H_2O (80:20 vol.%). We assume that even in a DMSO/water mixture, superoxide forms either directly ($O_2 + e \rightarrow O_2^{\bullet -}$), or *via* an intermediary complex of singlet oxygen and polythiophene (oligothiophenes) ($PT + h\nu \rightarrow PT^{\bullet} \rightarrow + O_2 \rightarrow [PT^{+\delta} .... {}^1O_2^{-\delta}] \rightarrow PT^{\bullet +} + O_2^{\bullet -}$), as has been reported[13]. Figure 3 shows that the EPR signal of the oxidized TEMP (TEMPO) grows under given experimental conditions only during the first 30 min of irradiation. We could show[13] that in

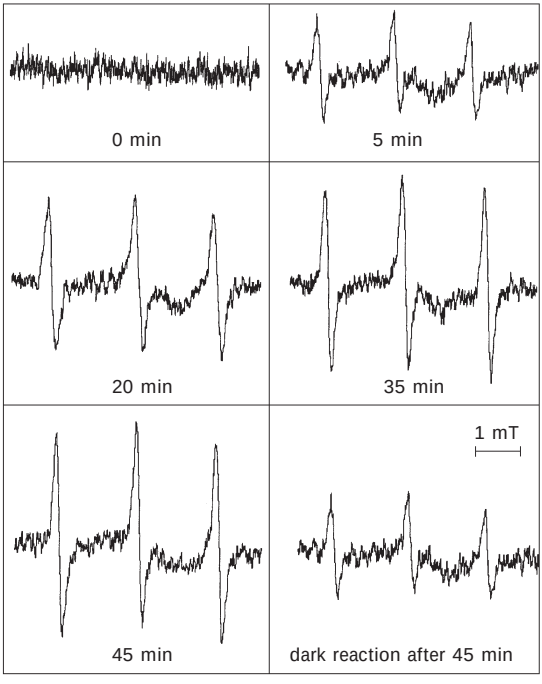

FIG. 3
Time-dependent photogeneration of $O_2^{\bullet -}$, monitored by spin-trapping agent TEMP (1.4×10^{-4} mol dm^{-3}) in a DMSO/water mixture (80:20 vol.%) and in the presence of 10 mg of zeolite photocatalyst

purely aqueous suspensions of modified zeolite, consecutive reactions of superoxide failed to generate the $^{\bullet}OH$ radical. Now we have designed an indirect method, in which we irradiate ($\lambda > 400$ nm) in DMSO/water mixtures (50:50, 70:30, 80:20, 90:10 vol.%) in the presence of DMPO and the photocatalyst. Whilst the 50:50 aqueous DMSO failed to show clear growth of EPR signal during irradiation, growth was observed in the 80:20 vol.% mixture. Figure 4a shows such EPR spectrum of the mixture of 10 mg of photocatalyst – Fe-ZSM-5-polythiophene, 900 μl DMSO, 100 μl water and 40 μl DMPO as superposition of several DMPO adducts with various radicals, generated during decomposition of DMSO and water in the subsequent dark reactions. Out of radicals possibly generated during irradiation, we could identify at least four species, adducts of DMPO with intermediary radicals, possessing the following splitting constants: $^{\bullet}OH$ with $a_N = a_H = 1.68$ mT; $CH_3OO^{\bullet}$ with $a_N = 1.3$ mT, $a_H = 0.8$ mT; $CH_3O^{\bullet}$ with $a_N = 1.34$ mT, $a_H = 1.16$ mT; DMPOX$^{\bullet}$ with $a_N = 1.34$ mT and/or DMPO–$O_2^{\bullet-}$ with $a_N = 1.41$ mT, $a_H = 1.14$ mT. For instance, hydroxyl radicals can be generated by the following reactions[15]:

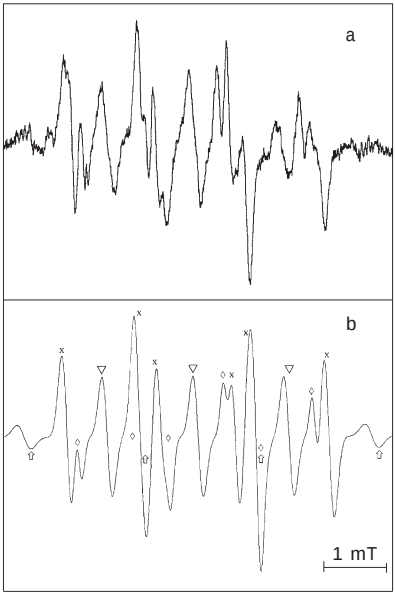

FIG. 4

EPR spectrum of a mixture of 10 mg photocatalyst, 900 μl DMSO, 100 μl water and 40 μl DMPO (3.4×10^{-4} mol dm^{-3}) after 5 min irradiation ($\lambda > 400$ nm) (a); simulated spectrum of adducts with DMPO (↓ DMPO–HO$^{\bullet}$, ◊ DMPO–$CH_3OO^{\bullet}$, × DMPO–$CH_3O^{\bullet}$, ▽ DMPOX$^{\bullet}$) (b)

$$2\ O_2^{\bullet -} + 2\ H^+ \rightarrow O_2 + H_2O_2$$

$$H_2O_2 + e \rightarrow {}^{\bullet}OH + OH^-$$

$$OH^- + PT^{\bullet +} \rightarrow {}^{\bullet}OH + PT$$

Hydroxyl radicals react very quickly with DMSO forming methyl radicals[16]. On the other hand, methyl radicals may react immediately with molecular oxygen forming $CH_3OO^{\bullet}$ radicals[17,18]. The values of splitting constants a_N and a_H match those reported for such adducts in the database of EPR spectra[19]. Using Bruker software (WINEPR, SymFonia), we simulated the spectra of the above four adducts (Fig. 4b), and found them to be in good agreement with the experimental spectra. The observed deviations of theoretical spectrum from experiment probably account for the presence of DMPO ad-

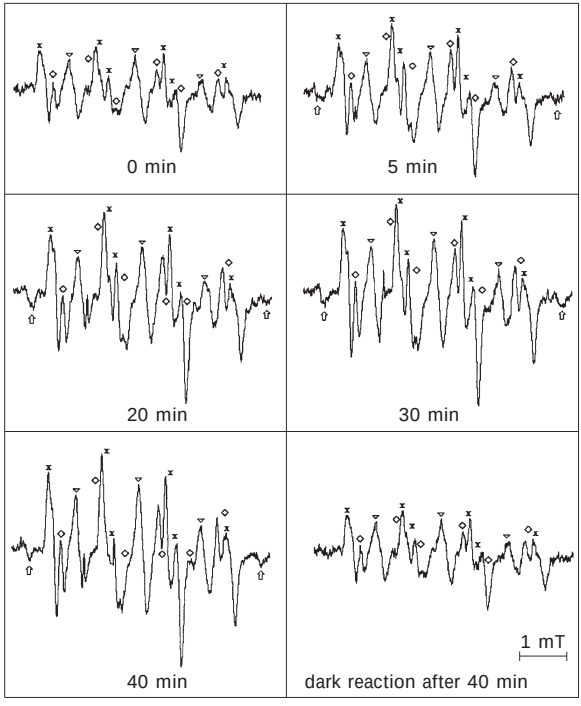

FIG. 5
Time-dependent EPR signal of adducts of DMPO with $^{\bullet}OH$ (↓), $CH_3OO^{\bullet}$ (◊), $CH_3O^{\bullet}$ (×), and $X^{\bullet}$ (▽) in a mixture of 10 mg of photocatalyst, 900 μl DMSO, 100 μl H_2O and 40 μl DMPO (3.4×10^{-4} mol dm^{-3}). All spectra were registered at the same amplification

ducts with other radicals, *e.g.* $O_2^{\bullet -}$, which possess similar splitting constants as the above-mentioned four radical species (for instance DMPO–$O_2^{\bullet -}$ has a_N = 1.41 mT, a_H = 1.14 mT)[19]. Such reasoning can be corroborated by the fact, that the presence of $O_2^{\bullet -}$ was detected also by TEMP [13].

During irradiation with visible light, the concentrations of respective adducts grow (Fig. 5), with the concentration of the $CH_3OO^{\bullet}$–DMPO adduct growing in the first phase (first 10 min) faster than the others. When TEMP was used as a spin-trapping agent, the EPR signals also grew, confirming the role of light in the generation of radicals (Fig. 3).

Time-dependent EPR spectra show that after the initial 10 min the signal intensity of the DMPO–$CH_3OO^{\bullet}$ or DMPO–$O_2^{\bullet -}$ adduct decreases, whereas that of the DMPO–$CH_3O^{\bullet}$ adduct keeps growing (Fig. 5). The time-dependence of EPR spectra can be accounted for by assuming that in the mixture of photocatalyst, DMSO, water and DMPO, $^{\bullet}OH$ radicals and other ROS species are generated even in the ensuing dark reactions. Their subsequent reactions with DMSO then generate $CH_3OO^{\bullet}$ radicals, which in turn immediately attack DMPO (hence higher intensity of the corresponding EPR signals in the first phase of reaction). Further irradiation converts the $CH_3OO^{\bullet}$ radical into $CH_3O^{\bullet}$, causing depletion of DMPO–$CH_3OO^{\bullet}$ and growth of the DMPO–$CH_3O^{\bullet}$ signal.

Transformation of the $CH_3OO^{\bullet}$ radical to methoxy radicals $CH_3O^{\bullet}$ can be easily observed also in the dark reaction of the studied mixture (Fig. 6). We

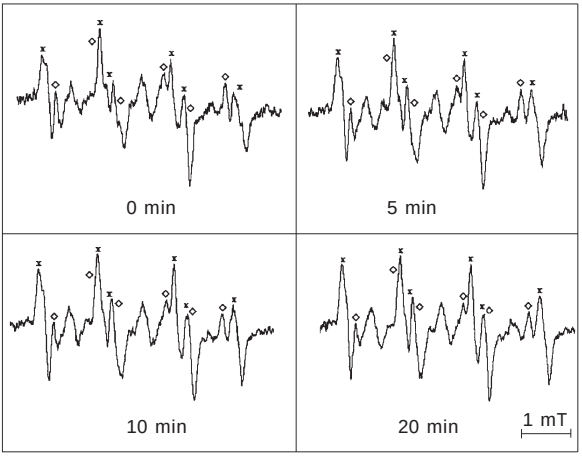

FIG. 6

Time-dependent EPR signal of adducts of DMPO with $^{\bullet}OH$ (↓), $CH_3OO^{\bullet}$ (◊), $CH_3O^{\bullet}$ (×), $X^{\bullet}$ (▽) generated in dark reactions in a mixture of 10 mg of photocatalyst, 900 μl DMSO, 100 μl H_2O and 40 μl DMPO (3.4×10^{-4} mol dm^{-3}). All spectra were registered at the same amplification

can see clearly the decreasing intensity of the $CH_3OO^{\bullet}$ adduct signal with time. Interestingly, the DMPO–$HO^{\bullet}$ adduct has not been recorded, probably due to fast consumption of $^{\bullet}OH$ radicals in the transformations to methylperoxy and methoxy radical intermediates.

Having confirmed generation of $^{\bullet}OH$ radical in the photoreaction, we set out to investigate the possibility of first dechlorination and possible deeper degradation of selected aromatic compounds. At first we used 4-chlorophenol, a known contaminant of the environment. Its photooxidation has been known to produce in the first phase phenol and hydroquinone[20]; the primary products can further mineralize. Figure 7 shows time-dependent

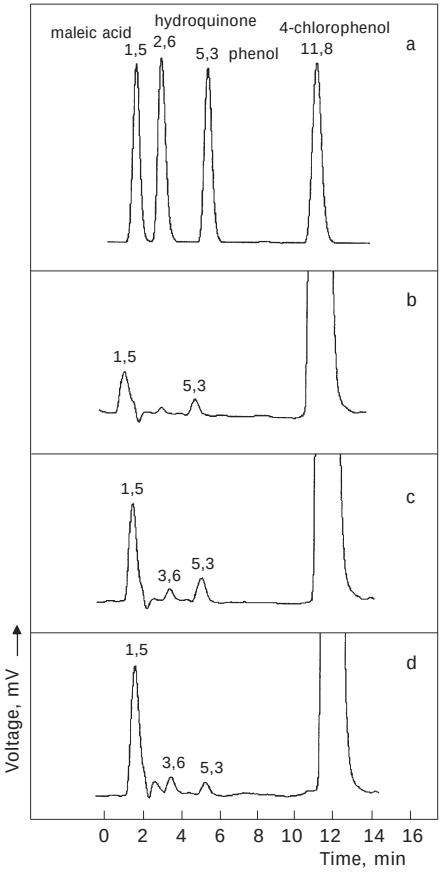

FIG. 7

Time-dependent HPLC chromatogram of 4-chlorophenol (2.5×10^{-3} mol dm^{-3}) irradiated in aqueous suspension of photocatalyst (250 mg in 250 cm^3 water, pH 5.6): standards of degradation products (a); 2 (b), 4 (c) and 8 h (d) after irradiation ($\lambda > 400$ nm)

HPLC chromatograms, documenting the concentration growth of four main products of irradiation ($\lambda > 400$ nm) in purely aqueous media in the presence of a photocatalyst. Standard compounds were used to prove a formation of phenol, hydroquinone, maleic acid and an unidentified compound with the retention time of 3.6 min as primary degradation products. If we assume validity of the known mechanism of ring-opening of hydroquinone and catechol, compounds generated by addition of the $^{\bullet}OH$ radical to phenol are maleic or muconic acid[21] and the unidentified compound can be either catechol or product of its ring-opening.

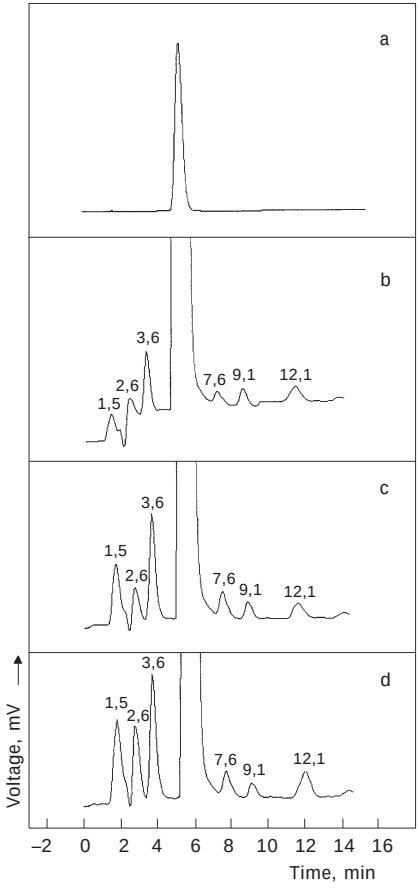

FIG. 8

Time-dependent HPLC chromatogram of phenol (2.5×10^{-3} mol dm^{-3}) irradiated in aqueous suspension of photocatalyst (250 mg of photocatalyst in 250 cm^3 water, pH 5.6): irradiation time 0 (a), 2 (b), 4 (c) and 8 h (d) ($\lambda > 400$ nm)

Degradation of 4-chlorophenol continues, even after dechlorination was confirmed, by irradiation of phenol under identical experimental conditions. Formation of products during irradiation of aqueous solution of phenol in the presence of photocatalyst is shown in Fig. 8. In the presence of $^{\bullet}OH$ radicals, all main primary degradation products found in irradiation of 4-chlorophenol are formed. Differences in relative concentrations of degradation "products" are probably a manifestation of different distribution of active sites on the respective photocatalysts, or due to the fact that photodegradation of 4-chlorophenol may be accompanied by changes in pH caused by released hydrochloric acid[22]. The effect of distribution of active sites of the photocatalysts, both in the entrance of the channels and, on its surface on the kinetics of photodegradation will be the object of further studies.

CONCLUSIONS

1. Photooxidative oligomerization of thiophene in the channels of zeolite Fe^{3+}-ZSM-5 affords a photocatalyst absorbing in the visible part of spectrum ($\lambda > 400$ nm) and suitable for photodegradation of 4-chlorophenol in aqueous media.

2. It can be assumed that $^{\bullet}OH$ radical participates in the photodegradation; its presence has been confirmed by spin-trapping (DMPO) in a DMSO/water mixture.

3. Irradiation of 4-chlorophenol with visible light generates, in aqueous suspension of the generated photocatalyst, three main products: phenol, hydroquinone, and maleic acid. Ring-opening of phenol was confirmed by independent irradiation of phenol.

The work has been supported by the Ministry of Education of the Slovak Republic (grant No. 1/8109/01).

REFERENCES

1. Olins D. F., Al-Ekabi H. (Eds): *Proc. 1st Int. Conference on TiO_2, London, Ontario, Canada, November 8–13, 1992*. Amsterdam–London–New York–Tokyo 1992.
2. Hofmann M. R., Martin S. T., Choi W., Bahnemann D. F.: *Chem. Rev. (Washington, D. C.)* **1995**, *95*, 69.
3. Chatterjee D., Mahata A.: *Catal. Commun.* **2001**, *2*, 1.
4. Fan F.-R. F., Bard A. J.: *J. Am. Chem. Soc.* **1979**, *101*, 6139.
5. Lin G., Li X., Zhao J., Horikoshi S., Hidaka H.: *J. Mol. Catal., A* **2000**, *153*, 221.
6. Illiev V.: *J. Photochem. Photobiol., A* **2002**, *151*, 195.

7. Shibata T., Kabumoto A., Shiragami T., Ishitani O., Pac C., Yanagida S.: *J. Phys. Chem.* **1990**, *94*, 2068.
8. Matsuoka S., Kohzuki T., Nakamura A., Pac C., Yanagida S.: *J. Chem. Soc., Chem. Commun.* **1991**, 580.
9. Yamamoto T., Yoneda Y., Maruyama T.: *J. Chem. Soc., Chem. Commun.* **1992**, 1652.
10. Hasegawa K., Weng C., Kotani T., Kanbara T., Kagaya S., Yamamoto T.: *J. Mater. Soc. Lett.* **1999**, *18*, 1091.
11. Wen C., Hasegawa K., Kanbara T., Kagaya S., Yamamoto T.: *J. Photochem. Photobiol., A* **2000**, *137*, 45.
12. Wen C., Hasegawa K., Kanbara T., Kagaya S., Yamamoto T.: *J. Photochem. Photobiol., A* **2000**, *133*, 59.
13. Čík G., Šeršeň F., Bumbálová A.: *Collect. Czech. Chem. Commun.* **1999**, *64*, 149.
14. Čík G., Hubinová M., Šeršeň F., Brezová V.: *Collect. Czech. Chem. Commun.* **2002**, *67*, 1743.
15. Čík G., Šeršeň F., Bumbálová A.: *Microporous Mesoporous Mater.* **2001**, *46*, 81.
16. Veltwich D., Janata E., Asmus K.-D.: *J. Chem. Soc., Perkin Trans.* **1980**, *2*, 146.
17. Marchaj A., Kelley D. G., Bakac A., Espenson J. H.: *J. Phys. Chem.* **1991**, *95*, 4440.
18. Sauer A., Cohen H., Meyerstein D.: *Inorg. Chem.* **1989**, *28*, 2511.
19. Anson S. W., Li A. S. W., Cummings K. B., Roethling H. P., Buettner G. R., Chignell C. F.: A Spin Trapping Database Implemented on the IBM PC/AT, *J. Magn. Reson.* **1988**, *79*, 140; http://epr.niehs.nih.gov/.
20. Da Silva J. P., Ferreira L. F. V., DaSilva A. M., Oliveira A. S.: *J. Photochem. Photobiol., A* **2002**, *151*, 157.
21. Santos A., Yustos P., Quintanilla A., Rodríguez S., García-Ochoa F.: *Appl. Catal., B* **2002**, *39*, 97.
22. Mills A., Wang J.: *J. Photochem. Photobiol., A* **1998**, *118*, 53.